Title

New In Vitro Model To Study the Effect of Human Simulated Antibiotic Concentrations on Bacterial Biofilms

Journal

Antimicrobial Agents and Chemotherapy, 59(7)

ISSN

0066-4804

Authors

Haagensen, Janus AJ
Verotta, Davide
Huang, Liusheng
et al.

Publication Date

2015-07-01

DOI

10.1128/aac.05037-14

Peer reviewed

AAC Journals.ASM.org

New *In Vitro* Model To Study the Effect of Human Simulated Antibiotic Concentrations on Bacterial Biofilms

Janus A. J. Haagensen,[b] Davide Verotta,[c] Liusheng Huang,[a] Alfred Spormann,[b] Katherine Yang[a]

Department of Clinical Pharmacy, University of California San Francisco School of Pharmacy, San Francisco, California, USA[a]; Department of Civil and Environmental Engineering, Stanford University, Stanford, California, USA[b]; Department of Bioengineering and Therapeutic Sciences, University of California San Francisco School of Pharmacy, San Francisco, California, USA[c]

A new *in vitro* pharmacokinetic/pharmacodynamic simulator for bacterial biofilms utilizing flow cell technology and confocal laser scanning microscopy is described. The device has the ability to simulate the changing antibiotic concentrations in humans associated with intravenous dosing on bacterial biofilms grown under continuous culture conditions. The free drug concentrations of a single 2-g meropenem intravenous bolus dose and first-order elimination utilizing a half-life of 0.895 h (elimination rate constant, 0.776 h^{-1}) were simulated. The antibacterial activity of meropenem against biofilms of *Pseudomonas aeruginosa* PAO1 and three clinical strains isolated from patients with cystic fibrosis was investigated. Additionally, the effect of meropenem on PAO1 biofilms cultured for 24 h versus that on biofilms cultured for 72 h was examined. Using confocal laser scanning microscopy, rapid biofilm killing was observed in the first hour of the dosing interval for all biofilms. However, for PAO1 biofilms cultured for 72 h, only bacterial subpopulations at the periphery of the biofilm were affected, with subpopulations at the substratum remaining viable, even at the conclusion of the dosing interval. The described model is a novel method to investigate antimicrobial killing of bacterial biofilms using human simulated concentrations.

Microbial biofilms have been implicated in virtually every human infection, ranging from common outpatient infections, such as otitis media and sinusitis, to severe or life-threatening infections, including orthopedic implant infections, catheter-related bloodstream infections, endocarditis, and cystic fibrosis (CF). Biofilm-mediated infections due to *Staphylococcus aureus* and *Pseudomonas aeruginosa* are particularly costly and difficult to treat and have been classified as serious threats to human health by the United States Centers for Disease Control and Prevention and the Infectious Diseases Society of America (1, 2). Cystic fibrosis, in particular, is characterized by chronic and repeated lung infections with *Pseudomonas aeruginosa*. *P. aeruginosa* resides as biofilms in the lungs of CF patients, where it undergoes extensive genetic and adaptive changes, allowing it to survive and persist, despite repeated courses of antibiotic therapy (3). Once *P. aeruginosa* is established in the airway of CF patients, eradication of *P. aeruginosa* is nearly impossible. The difficulty in treating biofilm infections is further compounded by the lack of new antibacterial agents in the developmental pipeline (4). Thus, there is a significant need to optimize the dosing of currently available agents (5, 6).

Bacterial biofilms have been shown to be 100 to 1,000 times more antibiotic resistant/tolerant than planktonic, or free-swimming, bacteria. However, planktonic cells derived from biofilm cells remain fully susceptible to antibiotics (7). Thus, there is a poor correlation between traditional antibiotic testing methods (e.g., determination of the MIC) and clinical and microbiological outcomes in the treatment of biofilm infections (8). Moreover, current *in vitro* pharmacokinetic (PK) and pharmacodynamic (PD) investigations focus on bacteria grown under conditions most appropriate for planktonic cells (e.g., liquid culture), which lack the complexity of heterogeneity in structure, composition, physiology, and metabolism experienced by biofilm cells and which are known to contribute significantly to antimicrobial resistance/tolerance. On the basis of PK/PD studies with planktonic bacteria, all antibiotics are known to exhibit either time-dependent killing (e.g., β-lactams) or concentration-dependent killing (e.g., aminoglycosides and fluoroquinolones) for efficacy (9). For antibiotics that exhibit time-dependent killing, such as β-lactams, the percentage of time that the free drug concentration exceeds the MIC (percent fT_{MIC}) during a dosing interval is most predictive of clinical or microbiological efficacy. Meropenem, a carbapenem antibiotic, requires a PD target of ~40% for bactericidal activity (10, 11). For aminoglycosides, the ratio of the maximum concentration in serum (C_{max}) to the MIC (C_{max}/MIC) is most predictive of microbial killing; for fluoroquinolones, it is the ratio of the area under the concentration-time curve (AUC) to the MIC (AUC/MIC) (12, 13). It is unknown if these indices are applicable to bacteria residing in biofilms. As a result, the optimal dose of antibiotic needed to eradicate biofilm-mediated infections, such as orthopedic implant infections or cystic fibrosis, is largely unknown.

In vitro PD modeling studies are important first steps in the preclinical analysis of antibiotics. Static models utilize set inocula of bacteria grown in fixed antibiotic concentrations in 96-well microtiter trays (14–16). Dynamic models, however, have the advantage of mimicking human physiologic drug concentrations as-

Received 15 December 2014 **Returned for modification** 15 February 2015
Accepted 20 April 2015

Accepted manuscript posted online 27 April 2015

Citation Haagensen JAJ, Verotta D, Huang L, Spormann A, Yang K. 2015. New *in vitro* model to study the effect of human simulated antibiotic concentrations on bacterial biofilms. Antimicrob Agents Chemother 59:4074–4081. doi:10.1128/AAC.05037-14.

Address correspondence to Katherine Yang, yangk@pharmacy.ucsf.edu.

doi:10.1128/AAC.05037-14

sociated with drug delivery, penetration, metabolism, and elimination. Dynamic planktonic cell models have been in existence since the 1970s and range from simple dilution models to hollow-fiber infection models (14). In a one-compartment dilution model, a simple suspension of planktonic bacteria is used to simulate the site of infection in a central compartment (typically, a flask). The antibiotic is added to this central compartment at a fixed rate to simulate the first-order elimination kinetics. Because biofilm bacteria require a surface for adherence, sampling of the liquid bacterial medium in these models results in testing of only the planktonic bacteria suspended in the liquid medium or bacterial mutants that are defective in biofilm formation, leaving the biofilm cells remaining adherent to the flask. Additionally, biofilm pattern formation is highly variable, depending on the availability of nutrients, shear stress, temperature, and the surface to which they adhere. This heterogeneity in pattern formation facilitates the survival of one or more subpopulations and plays an important role in antibiotic resistance/tolerance (17). While multiple dynamic systems for the study of biofilms have been developed, flow-based systems using flow cell technology and confocal laser scanning microscopy (CLSM) are considered the "gold standard" (18, 19). Flow cell systems with CLSM have the advantage of allowing insight into the spatial organization and function of the three-dimensional biofilms in real time under noninvasive, continuous culture conditions down to the single-cell level. The present study describes a novel dynamic *in vitro* PK/PD model for investigating the effect of human simulated meropenem concentrations on *P. aeruginosa* biofilms grown under continuous-flow conditions.

MATERIALS AND METHODS

Bacterial strains and antibiotic testing. *P. aeruginosa* PAO1 and three isogenic clinical *P. aeruginosa* isolates were used (20, 21). The three isolates represent clone DK08 and were cultured from a single pediatric patient with repeated *P. aeruginosa* lung infection from the Copenhagen Cystic Fibrosis Center (21). The three isolates were sequentially cultured from samples from the patient at yearly intervals and are labeled DK08.1, DK08.2, and DK08.3. PAO1 was tagged with green fluorescent protein (GFP) as previously described (22). For each isolate, the MIC of meropenem for planktonic cells was determined by broth macrodilution and interpreted in accordance with a Clinical and Laboratory Standards Institute methodology (23). The biofilm inhibitory concentration (BIC) was determined utilizing the previously established biofilm susceptibility assay developed by Moskowitz et al. (15).

Antibiotic and medium. Meropenem for intravenous injection (50 mg/ml; lot number KA662; expiration date, March 2015; Astra Zeneca) was obtained from the pharmacy at the University of California San Francisco Medical Center. M9 minimal medium (Amresco, Solon, OH) supplemented with 1 mM $MgSO_4$, 0.1 mM $CaCl_2$, and 0.01 mM $FeCl_3$ was utilized for the biofilm experiments. An additional 10 mM glucose was added for static experiments (e.g., MIC and BIC determination); 0.3 mM glucose was utilized for flow chamber experiments (22).

Simulated meropenem concentrations. The free drug concentrations of a single 2-g meropenem intravenous dose over an 8-h period were simulated. Concentration-time profiles were based on previously described values of PK parameters from healthy volunteers (24). On the basis of the parameter values in the literature (24), the peak concentration was computed to be 107.53 mg/liter and the trough concentration at 8 h was 0.22 mg/liter.

***In vitro* PD biofilm model.** The one-compartment biofilm model is an adaptation of the planktonic dilution model first developed by Grasso et al. (25) and the flow cell models used to study bacterial biofilms (26).

A schematic of the model is shown in Fig. 1. A dilution flask, flask A, containing minimal medium was connected to a mixing flask, flask B (volume V_B) containing dose D of meropenem via a peristaltic pump (Watson Marlow 205S). Meropenem from flask B was connected to the bubble traps and flow chambers (FC) via the same peristaltic pump. *P. aeruginosa* biofilms were cultivated in the flow chambers distal to the bubble traps. Three independent bubble traps and flow chambers were connected to flask B by separate tubing to allow three experiments to run simultaneously. Bubble traps are used to minimize introduction of air bubbles into the flow chambers, which can disrupt the three-dimensional structure of the biofilm (26). The flow rate (F) at which diluent was pumped from flask A into flask B was equal to the rate at which antibiotic was pumped from flask B into the flow chambers ($F_{A\text{-}B} = F_{B\text{-}FC}$); thus, V_B remained constant. The tubing and bubble traps were initially primed with the peak concentration [$C_{(p)}$] of meropenem prior to the start of the experiment. At time zero, the pump was initiated and the antibiotic concentrations in flask B and the flow chambers decreased exponentially according to the equation $C_{(t)} = C_{(p)}e^{-k_{el}t}$, where $C_{(t)}$ is the concentration at time t, $C_{(p)}$ is the antibiotic concentration at time zero, and k_{el} is the elimination rate constant. k_{el} and the half-life ($t_{1/2}$) are functions of the F of the pump and V_B, such that k_{el} is equal to F/V_B and $t_{1/2}$ is equal to $0.693/k_{el}$, which is equal to $(0.693/F) \times V_B$. To simulate a $t_{1/2}$ of 0.893 h and a meropenem $C_{(p)}$ of 107.53 mg/liter while maintaining a constant flow rate of 20 ml/h per flow cell, a V_B of 25.82 ml was required. This volume was tripled to account for the fact that three flow chambers, corresponding to a final V_B of 77.46 ml, were run simultaneously. A magnetic stir bar in flask B ensured homogeneous mixing. Luer locks placed downstream of the flow chambers were used to obtain samples for determination of antibiotic concentrations throughout the experiment. The entire apparatus was incubated in a 30°C room in order to minimize temperature changes, which can introduce air bubbles into the system (27).

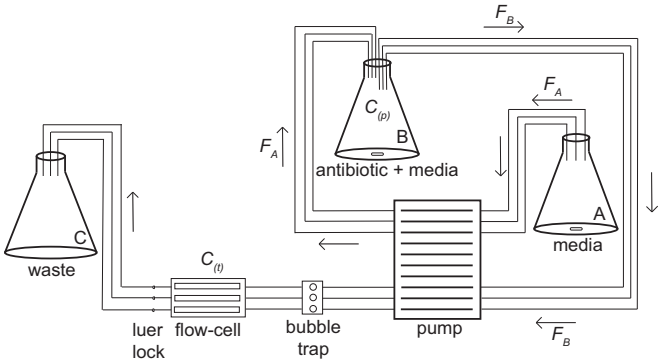

FIG 1 Diagram of the *in vitro* biofilm PK/PD model used to simulate a 2-g meropenem intravenous bolus and associated monoexponential drug decline, i.e., $C_{(t)} = C_{(p)}e^{-k_{el}t}$, where $C_{(t)}$ is the concentration at time t, $C_{(0)}$ is the initial concentration, k_{el} is the elimination rate constant, and t is time. F_A, flow rate from flask A to flask B; F_B, flow rate from flask B to the flow cell.

Cultivation of flow-supported *P. aeruginosa* biofilm. Prior to starting the meropenem, a *P. aeruginosa* biofilm was cultivated in each of the three flow chambers as previously described (26, 28). Strain PAO1 was cultivated for either 24 or 72 h, and each clinical isolate was cultivated for 24 h. In brief, each flow chamber was inoculated with 250 μl of an overnight culture of PAO1 or a clinical isolate diluted to an optical density at 600 nm of 0.05 and left without flow. After 1 h, the flow of minimal medium was initiated at the same flow rate described above (i.e., 20 ml/h). After cultivation for 24 or 72 h in the flow chambers, the pump was temporarily stopped and the tubing distal to the bubble traps was clamped. Minimal medium was replaced with flask B containing the $C_{(p)}$ of meropenem. The bubble traps were emptied, and all tubing and bubble traps were reprimed with the $C_{(p)}$ of meropenem. Flask A with minimal medium was connected to flask B, all tubing was unclamped, and flow was resumed at a rate of 20 ml/h, as described above. At the completion of

TABLE 1 Meropenem MICs and BICs for the *Pseudomonas aeruginosa* isolates used in the *in vitro* PK/PD device[a]

Isolate	MIC (mg/liter)	BIC (mg/liter)
PAO1	2	32
DK08.1	2	8
DK08.2	2	16
DK08.3	2	16

[a] BIC, biofilm inhibitory concentration. DK08.1, DK08.2, and DK08.3 represent sequential clinical isolates of clone DK08.

TABLE 2 Mean meropenem concentrations after administration of a single 2-g bolus over an 8-h period

Time (h)	Mean ± SEM concn[a] (mg/liter)				
	Mixing flask	Flow chamber 1	Flow chamber 2	Flow chamber 3	Target
0	104.34 ± 5.79	107.40 ± 1.72	105.40 ± 2.25	106.78 ± 2.45	107.53
0.5		76.82 ± 3.11	76.84 ± 3.53	75.82 ± 2.92	73.01
1		51.22 ± 2.33	51.04 ± 2.47	51.36 ± 2.40	49.58
2		23.06 ± 0.91	22.92 ± 1.02	23.10 ± 0.84	22.86
4	3.25 ± 0.68	4.62 ± 0.44	4.40 ± 0.37	4.41 ± 0.40	4.86
6		0.86 ± 0.11	0.94 ± 0.15	0.80 ± 0.09	1.03
8	0.11 ± 0.04	0.16 ± 0.03	0.16 ± 0.02	0.15 ± 0.02	0.22

[a] Means ± standard errors of the means (SEMs) were calculated from each flow chamber from experiments using 24-h-old strain PAO1, 72-h-old strain PAO1, and 24-h-old strain DK08.1, DK08.2, or DK08.3.

administration of the meropenem bolus, the 72-h-old biofilms were harvested from the flow chambers by rapidly injecting medium containing glass beads (diameter, 150 to 212 μm; Sigma) in and out of the flow chambers using syringes (29). The resultant bead-containing suspension was vortexed, and the MIC was determined using the resultant bacterial suspension, as previously described (23). The 24-h-old biofilms were not harvested, as the cells were effectively killed with a single dose; thus, there were no cells to harvest.

Antibiotic concentration determinations. Samples were taken from each flow chamber via the luer locks at times of 0, 0.5, 1, 2, 3, 4, 6, and 8 h and assayed for meropenem. All samples were immediately stored at −80°C until analyses. Samples were analyzed within 1 to 2 weeks by liquid chromatography-tandem mass spectrometry (LC-MS/MS) as previously described for minimal medium (30). During the course of sample analysis, quality control samples of 150 ng/ml ($n = 25$), 1,500 ng/ml ($n = 23$), 8,000 ng/ml ($n = 25$), and 100,000 ng/ml ($n = 30$) exhibited relative standard deviations (RSDs) ranging from 3.1% to 5.6% and intra-assay mean accuracies ranging from 94.4% to 107%.

Microscopy and image acquisition. Microscopic observations of the flow cells were completed using a Leica TCS SP2 CLSM equipped with an argon/krypton laser and detectors and filter sets for simultaneous monitoring of fluorescein isothiocyanate (FITC), Syto 9, and GFP (excitation, 488 nm; emission, 517 nm) for live cell staining and propidium iodide (excitation, 543 nm; emission, 565 nm) for dead cell staining. Images were obtained using a 40× Plan-Neofluar oil objective (numerical aperture, 1.3).

At time zero, the meropenem flow was initiated and images were taken at time zero and 0.5, 1, 2, 3, 4, 6, 8, and 24 h. Strain PAO1 and the clinical isolates were stained using the stain in the LIVE/DEAD BacLight bacterial viability kit (Molecular Probes, Invitrogen). Syto 9 and propidium iodide were injected into the tops of each bubble trap and allowed to flow into the flow chambers prior to image acquisition at each time point. Images were acquired at approximately 1-μm intervals in the *z* direction down through the biofilm. Two image stacks from random positions within the first centimeter of each flow chamber were acquired at each time point (a total of six images) to account for heterogeneity at different biofilm locations. Multichannel simulated fluorescence projections (SFPs) and sections through the biofilms were generated using Imaris software (Bitplane AG, Switzerland).

Statistical analyses. A monoexponential function of the form $(D/V)e^{-k_{el}t}$, where D is the meropenem dose, V is the volume of distribution, and k_{el} is the elimination rate constant, was fitted to the observed concentrations using the nonlinear modeling program NONMEM (version VII; Icon Development Solutions, Ellicott City, MD) to determine concentrations. A proportional error model was incorporated into the model following visual and trend analysis of the variances of the concentrations at different observation times. A nonlinear random effects model was used to evaluate interexperiment variability (31). Under this model the parameters V and k are assumed to be log-normally distributed with (interexperimental) variance that is estimated from the data.

RESULTS

Static antibiotic susceptibility testing. The results of the meropenem susceptibility tests performed with planktonic and biofilm cells in minimal medium prior to the flow chamber studies are shown in Table 1. The BIC for PAO1 was found to be 16 times higher than the corresponding MIC for planktonic cells. For the clinical strains, the BIC values were 4 to 8 times higher than the corresponding MIC values. After PAO1 was harvested from the flow chambers, the MIC values for 72-h-old PAO1 remained unchanged at 2 mg/liter.

***In vitro* simulation of meropenem.** The mean meropenem concentrations in each flow chamber after a single simulated 2-g meropenem intravenous bolus dose are shown in Table 2. The concentration-time profiles achieved using 24-h-old PAO1, 72-h-old PAO1, and the three clinical isolates are shown in Fig. 2. Minor deviations in concentration were observed between the 3 chambers. The modeling of the data showed no significant interexperiment (24 h versus 72 h) variability in k_{el} or V. Visual analysis of the residuals versus time for each flow chamber indicated a satisfactory fit with no unexplained trends. In addition, the fit of a biexponential model to the data did not show any improvement in the objective function value of the fit, confirming that a monoexponential model is appropriate to characterize the data. The estimated meropenem k_{el}s in each flow chamber obtained from the combined 24-h and 72-h experiments are shown in Table 3. Note the good approximation to the target k_{el}. The average apparent volume of distribution for the 3 chambers was 0.0187 liter. Table 4 reports the times above the target concentration (MIC or BIC) corresponding to the average V and the estimated k_{el} (0.797 h^{-1}) and the target k_{el} (0.776 h^{-1}).

Antimicrobial effect of meropenem on *P. aeruginosa* biofilm. CLSM images of the 24-h-old PAO1 biofilm throughout the 8-h dosing interval are shown in Fig. 3. After 24 h, a thin layer of cells, represented by the green cells, was observed in the flow chamber ($t = 0$ h). These cells form the initial microcolonies observed in early biofilm formation. The majority of the cells were killed within the first 4 h after antibiotic challenge and are represented by red cells. In contrast, PAO1 cells that were cultivated in the flow cell for 72 h formed complex biofilms with mushroom-shaped multicellular structures (Fig. 4). Over the 8-h dosing interval, differential killing of cells within the biofilm was observed. Biofilm subpopulations at the periphery of the biofilm exposed to the highest concentration of meropenem in the flow chambers (e.g., subpopulations closest to the fluid flowing in the chamber) were differentially killed first. These included the top layer of the biofilm and cells making up the multicellular cap. Subpopulations

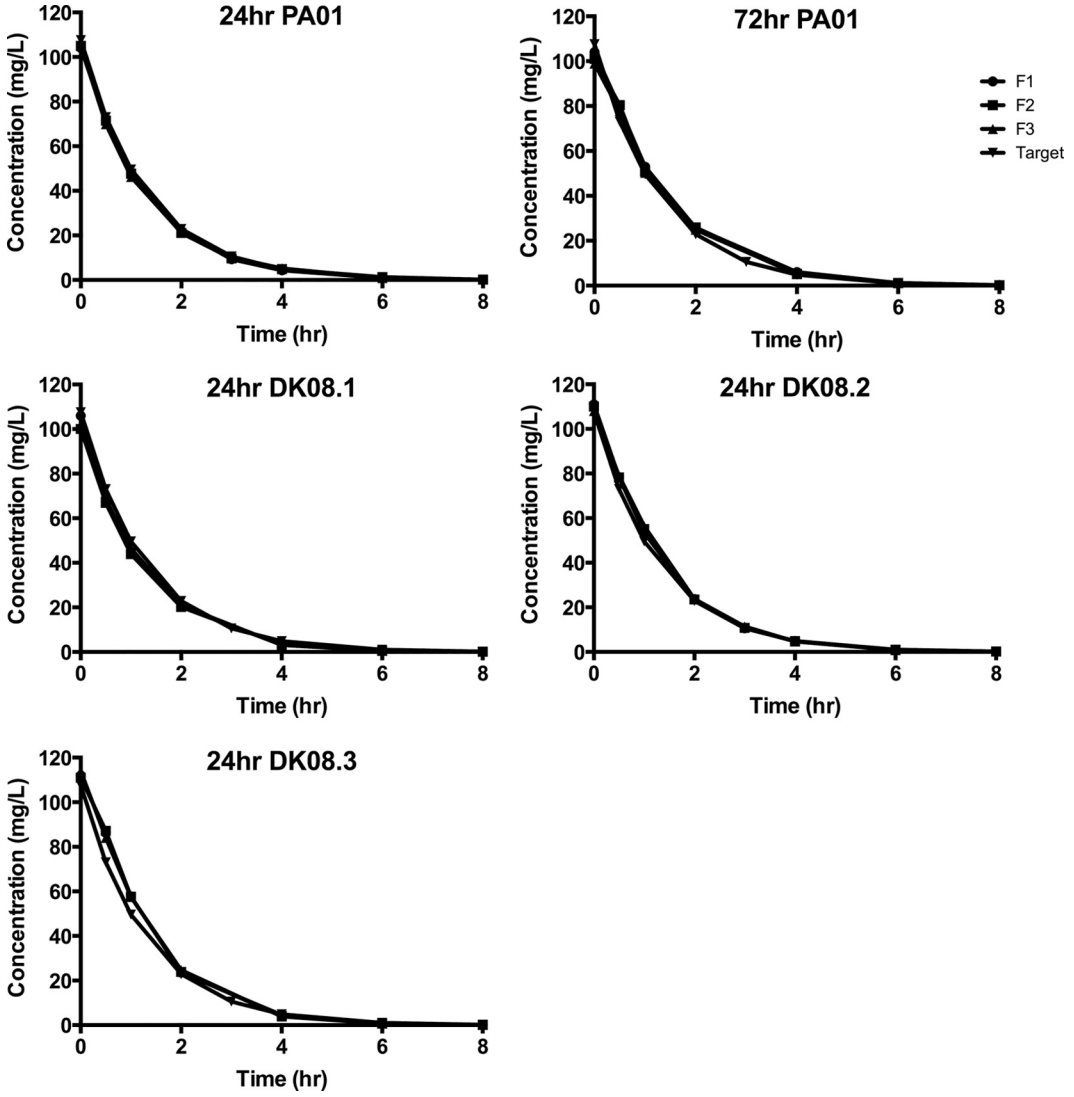

FIG 2 Concentration-time curve of a 2-g meropenem intravenous bolus achieved in each flow chamber for 24-h-old strain PAO1, 72-h-old strain PAO1, and three 24-h-old clinical strains (DK08.1, DK08.2, DK08.3). F1, flow chamber 1; F2, flow chamber 2; F3, flow chamber 3; Target, target concentration.

in the deeper compartments of the biofilm, such as the stalk of the colonies connected to the substratum, survived. At *t* equal to 4 h, cells deeper within the biofilm began to show susceptibility to meropenem treatment and were killed. However, even after the 8-h exposure to the simulated human dose, surviving cells were still detected at the substratum surface.

DISCUSSION

The described simulator is a novel device for assessing the effect of human simulated antibiotic concentrations on bacterial biofilms grown under continuous culture conditions. Biofilm pattern formation is known to be dependent on environmental conditions, such as nutrient and oxygen availability, carbon source, and the effect of the fluid flow (32–35). This presents unique challenges for the creation of a dynamic i*n vitro* PK/PD simulator, as the human simulated antibiotic concentrations are continuously

TABLE 3 Meropenem k_{el} after administration of a single 2-g bolus[a]

Component	Mean ± SE k_{el} (h^{-1})
Mixing flask	ND
Flow chamber 1	0.799 ± 0.018
Flow chamber 2	0.784 ± 0.017
Flow chamber 3	0.809 ± 0.015
Target	0.776

[a] k_{el}, elimination rate constant; ND, not done.

TABLE 4 Percent fT_{MIC} or BIC for *Pseudomonas aeruginosa* isolates used in the *in vitro* PK/PD device[a]

MIC or BIC (mg/liter)	Average estimated k_{el}		Target k_{el}	
	Time (h)	$\%fT_{MIC}$ or BIC	Time (h)	$\%fT_{MIC}$ or BIC
2	4.99	62.38	5.13	64.13
4	4.12	51.50	4.24	53.00
8	3.25	40.63	3.34	41.75
16	2.38	29.75	2.45	30.63
32	1.52	19.00	1.56	19.50

[a] BIC, biofilm inhibitory concentration; k_{el}, elimination rate constant; the percent fT_{MIC} or BIC is computed with respect to the concentration over an 8-h period.

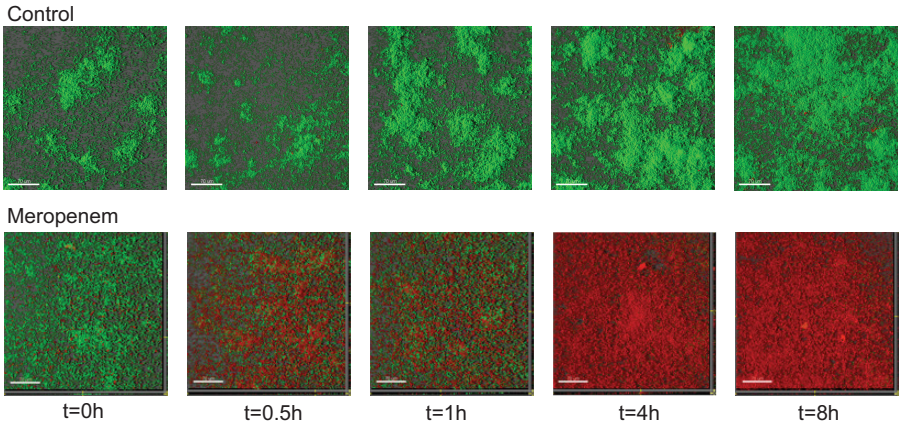

FIG 3 Effect of human simulated concentrations of a 2-g meropenem intravenous bolus on 24-h-old *P. aeruginosa* PAO1 grown in flow cells. CLSM images were acquired at time zero (prior to antibiotic administration) and 0.5, 1, 4, and 8 h. Control images are of the untreated flow chambers; meropenem images are of the meropenem-treated flow chambers. Red, dead cells after staining with propidium iodide. All *x-y* plots are presented as simulated fluorescence projections. Shown to the right of and below the *x-y* plots are vertical sections through the respective biofilm.

changing over time, while environmental factors, particularly the flow rate, must remain constant in order to correctly distinguish the effects of the antibiotic from those of the environment. Additionally, because the biofilms are adherent to a glass surface, conventional markers of antibiotic efficacy, such as cell counts (e.g., the number of CFU per milliliter), are not applicable, as traditional cell counts cannot be achieved without disrupting the structure of the biofilm. The use of CLSM allows the direct visualization of the differential killing of subpopulations within each layer of the biofilm over the course of the dosing interval, providing a three-dimensional representation of the PD of each drug.

For the preliminary tests of the simulator, *P. aeruginosa* was used as the model organism due to its clinical significance in biofilm-mediated infections, particularly in cystic fibrosis patients, and due to the extensive knowledge of the physiology of *P. aeruginosa* biofilms. The apparatus, however, can also be used to study other clinically significant biofilm-forming bacteria, such as *Staphylococcus aureus*, as well as the effect of antibiotics on mixed bacterial communities. Additionally, the device is not limited to the one-compartment pharmacokinetic model described in the present study but can also accommodate arbitrary pharmacokinetic profiles and alternative dosing strategies, such as extended or continuous infusions as well as multiple-antibiotic dosing. Meropenem, a carbapenem antibiotic, was chosen for the initial studies

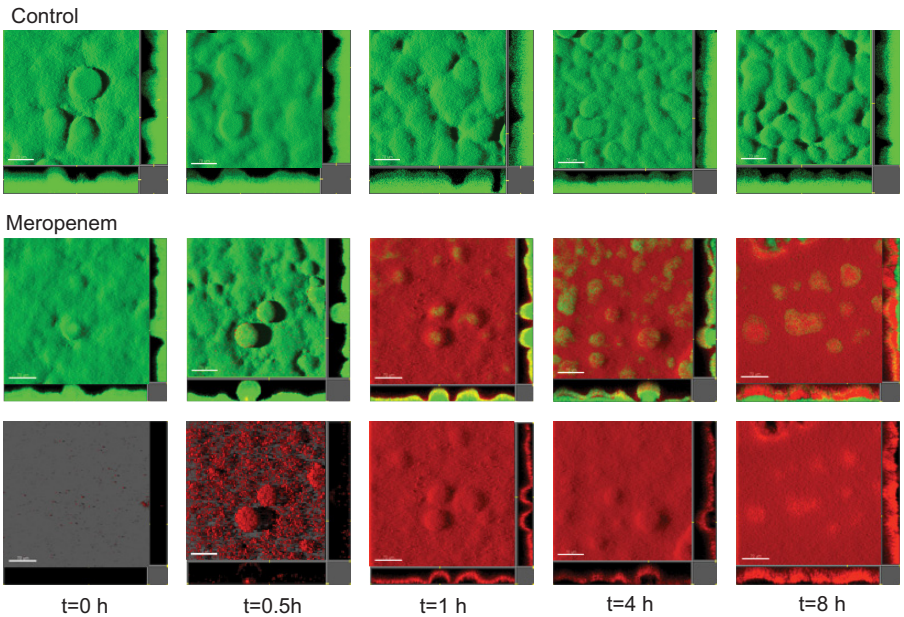

FIG 4 Effect of human simulated concentrations of a 2-g meropenem intravenous bolus on 72-h-old *P. aeruginosa* PAO1 grown in flow cells. CLSM images were acquired at time zero (prior to antibiotic administration) and 0.5, 1, 4, and 8 h. Control images are of the untreated flow chambers; meropenem images are of the meropenem-treated flow chambers. Red, dead cells after staining with propidium iodide. For the meropenem images, the top row represents live and dead cells and the bottom row represents dead cells only. All *x-y* plots are presented as simulated fluorescence projections. Shown to the right of and below the *x-y* plots are vertical sections through the respective biofilm.

because of its clinical application in the treatment of multidrug-resistant *P. aeruginosa*, particularly *P. aeruginosa* infections in the lungs of cystic fibrosis patients, and the human PK profile and planktonic cell PD parameters of meropenem have already been well described (10, 11, 24, 36–38). Future studies will include additional antibiotic classes targeting *P. aeruginosa*, including aminoglycosides and fluoroquinolones, as well as combination drug therapy targeting different spatial regions of the biofilm.

In the present studies, the PK/PD biofilm device closely modeled the human simulated meropenem concentrations typically achieved with a 2-g intravenous bolus dose on thin and thick biofilms. The need for determination of the pharmacodynamics of antibiotics on young and old biofilms was recently cited by the European Society for Clinical Microbiology and Infectious Diseases as an area of urgently needed research (8). Using the described model, a single meropenem bolus dose effectively killed cells within all strata of a thin 24-h-old PAO1 biofilm, most notably, within the first 4 h of antibiotic exposure. However, with a thicker 72-h-old biofilm, cells in the periphery of the biofilm and at the tops of the mushroom cap were differentially killed, while cells at the deeper substratum remained viable. This spatial response of a *P. aeruginosa* biofilm to meropenem confirmed previous observations and illustrates that PD indices and, thus, antimicrobial dosing are dependent upon the age of the biofilm. This may have important implications on antibiotic dose selection in acute versus chronic biofilm infections, such as infections in cystic fibrosis patients and orthopedic implant infections.

While it has been well established that bacteria residing in biofilms exhibit increased antimicrobial resistance compared to the resistance of the same bacteria grown in liquid culture, little is known regarding the PDs of antimicrobial agents on bacterial cells in biofilms. We report here that the BIC was 4 to 16 times higher than the corresponding MIC for planktonic cells, representing a clear decrease in the percent fT_{MIC} or BIC. While this is an important consideration for antimicrobial dosing, there is also clearly a differential response to antibiotics within different subpopulations in the biofilm. From the CLSM images, the PAO1 biofilms cultured for 72 h exhibit increased tolerance compared to that of the PAO1 biofilms cultured for 24 h, with increased amounts of residual live bacteria remaining in the flow chambers after a single dose. Additionally, the MIC of the 72-h-old cells harvested at the end of the meropenem dose was unchanged from the original MIC prior to antibiotic treatment, indicating that the viable cells were not a result of antibiotic resistance development. Instead, these cells likely represent persister cells within the biofilm (39). These persister cells recalcitrant to antibiotics that emerge then serve as a reservoir of surviving pathogens which are responsible for recurrent infections and therapeutic failures.

This spatial response to antibiotic treatment has been previously documented and is likely multifactorial. Oxygen and nutrient concentrations and, thus, metabolic activity are the highest at the outer surface of the biofilm and low in the center of the biofilm, leading bacteria to enter a nongrowing or stationary phase in the deeper portions of the biofilm (40). This is of particular importance, as most antibiotics require bacteria to be active and/or dividing in order to exert their antimicrobial effect. Tobramycin, ciprofloxacin, and β-lactam antibiotics kill bacteria at the biofilm perimeter (41–43). Colistin, a polymyxin antibiotic, does not require cells to be actively dividing and preferentially kills biofilm cells in the microcolony stalk, which exhibit low metabolic activity (22, 43). Antimicrobial resistance, analogously, is also differentially expressed within the biofilm in response to antibiotic exposure. Imipenem is known to be a strong inducer of the AmpC β-lactamase, while ceftazidime has been shown to be a weak inducer. Exposure to ceftazidime or subtherapeutic concentrations of imipenem resulted in the differential induction of AmpC β-lactamases only at the periphery of the biofilm, while subpopulations in the center of the microcolonies were not induced. However, at high imipenem concentrations, AmpC induction occurred in subpopulations throughout the biofilm (44). While colistin is active against nondividing cells in the deeper layers of the biofilm, colistin exposure leads to increased expression at the biofilm surface of the multidrug efflux pump MexAB-OprM, which plays a role in resistance to multiple antibiotic classes, including β-lactams, aminoglycosides, colistin, and fluoroquinolones (45–47). The PK/PD simulator, in conjunction with CLSM, is ideal for evaluating antimicrobial response and the development of antimicrobial tolerance under controlled conditions in real time using physiologic antibiotic concentrations associated with human dosing.

The *in vitro* PK/PD simulator does have certain limitations. While flow cell technology with CLSM is considered the gold standard for studying biofilm physiology, no *in vitro* model can fully mimic the complexity of *P. aeruginosa* lung infection in patients with cystic fibrosis and biofilms grown *in vitro* on a glass slide may differ from biofilms formed *in vivo*. However, *in vitro* models are widely utilized and recognized as a necessary first step in any preclinical antimicrobial PD analysis (48, 49). Additionally, in these preliminary experiments, only the human simulated concentrations of the elimination phase of the 2-g meropenem intravenous bolus were modeled. The absorption phase associated with a typical 30-min infusion was omitted for ease.

The *in vitro* PK/PD simulator for biofilm bacteria is useful for assessing the spatial and temporal effects of human antibiotic concentrations on bacterial biofilms. Biofilm infections, such as lung infections, orthopedic implant infections, and catheter-related infections, are significant causes of morbidity and mortality and result in high costs to the health care system. *In vitro* simulations, such as the one described in this study, will provide a better understanding of the response of biofilm infections to antibiotics that may improve clinical dosing of antimicrobial agents. In the case of patients with cystic fibrosis, *P. aeruginosa* cells reside in the lung primarily as bacterial biofilms. Thus, performance of PD studies on the predominant biofilm lifestyle mode may be more clinically relevant than the use of planktonic cell models. While the optimal planktonic cell PD indices for antibiotics are already known, the optimal biofilm PD indices are not. A more thorough understanding of the PDs of antibiotics on bacterial biofilms is a necessary first step in designing optimal antibiotic regimens to treat these infections.

ACKNOWLEDGMENTS

This work was supported by grant number 1R01 AI097380-0121 from the National Institute of Allergy and Infectious Diseases of the National Institutes of Health.

The clinical strains were kindly provided by Søren Molin and Helle Krogh Johansen at the Technical University of Denmark.

REFERENCES

1. **Spellberg B, Guidos R, Gilbert D, Bradley J, Boucher HW, Scheld WM,**

Bartlett JG, Edwards J, Jr, Infectious Diseases Society of America. 2008. The epidemic of antibiotic-resistant infections: a call to action for the medical community from the Infectious Diseases Society of America. Clin Infect Dis **46:**155–164. http://dx.doi.org/10.1086/524891.

2. **Centers for Disease Control and Prevention.** 2013. Antibiotic threats in the United States. Centers for Disease Control and Prevention, Atlanta, GA. http://www.cdc.gov/drugresistance/threat-report-2013/index.html.
3. **Ciofu O, Tolker-Nielsen T, Jensen PO, Wang H, Hoiby N.** 2 December 2014. Antimicrobial resistance, respiratory tract infections and role of biofilms in lung infections in cystic fibrosis patients. Adv Drug Deliv Rev http://dx.doi.org/10.1016/j.addr.2014.11.017.
4. **Boucher HW, Talbot GH, Benjamin DK, Bradley J, Guidos RJ, Jones RN, Murray BE, Bonomo RA, Gilbert D, Infectious Diseases Society of America.** 2013. 10 × ′20 progress—development of new drugs active against gram-negative bacilli: an update from the Infectious Diseases Society of America. Clin Infect Dis **56:**1685–1694. http://dx.doi.org/10.1093/cid/cit152.
5. **Society for Healthcare Epidemiology of America, Infectious Diseases Society of America, Pediatric Infectious Diseases Society.** 2012. Policy Statement on Antimicrobial Stewardship by the Society for Healthcare Epidemiology of America (SHEA), the Infectious Diseases Society of America (IDSA), and the Pediatric Infectious Diseases Society (PIDS). Infect Control Hosp Epidemiol **33:**322–327. http://dx.doi.org/10.1086/665010.
6. **Lodise TP, Lomaestro BM, Drusano GL.** 2006. Application of antimicrobial pharmacodynamic concepts into clinical practice: focus on beta-lactam antibiotics: insights from the Society of Infectious Diseases Pharmacists. Pharmacotherapy **26:**1320–1332. http://dx.doi.org/10.1592/phco.26.9.1320.
7. **Lewis K.** 2007. Persister cells, dormancy and infectious disease. Nat Rev Microbiol **5:**48–56. http://dx.doi.org/10.1038/nrmicro1557.
8. **Hoiby N, Bjarnsholt T, Moser C, Bassi GL, Coenye T, Donelli G, Hall-Stoodley L, Hola V, Imbert C, Kirketerp-Moller K, Lebeaux D, Oliver A, Ullmann AJ, Williams C, ESCMID Study Group for Biofilms, Consulting External Expert Werner Z.** 14 January 2015. ESCMID guideline for the diagnosis and treatment of biofilm infections 2014. Clin Microbiol Infect http://dx.doi.org/10.1016/j.cmi.2014.10.024.
9. **MacGowan AP.** 2001. Role of pharmacokinetics and pharmacodynamics: does the dose matter? Clin Infect Dis **33**(Suppl 3)**:**S238–S239. http://dx.doi.org/10.1086/321855.
10. **Nicolau DP.** 2008. Pharmacokinetic and pharmacodynamic properties of meropenem. Clin Infect Dis **47**(Suppl 1)**:**S32–S40. http://dx.doi.org/10.1086/590064.
11. **Turnidge JD.** 1998. The pharmacodynamics of beta-lactams. Clin Infect Dis **27:**10–22. http://dx.doi.org/10.1086/514622.
12. **Freeman CD, Nicolau DP, Belliveau PP, Nightingale CH.** 1997. Once-daily dosing of aminoglycosides: review and recommendations for clinical practice. J Antimicrob Chemother **39:**677–686. http://dx.doi.org/10.1093/jac/39.6.677.
13. **Forrest A, Nix DE, Ballow CH, Goss TF, Birmingham MC, Schentag JJ.** 1993. Pharmacodynamics of intravenous ciprofloxacin in seriously ill patients. Antimicrob Agents Chemother **37:**1073–1081. http://dx.doi.org/10.1128/AAC.37.5.1073.
14. **Gloede J, Scheerans C, Derendorf H, Kloft C.** 2010. In vitro pharmacodynamic models to determine the effect of antibacterial drugs. J Antimicrob Chemother **65:**186–201. http://dx.doi.org/10.1093/jac/dkp434.
15. **Moskowitz SM, Foster JM, Emerson J, Burns JL.** 2004. Clinically feasible biofilm susceptibility assay for isolates of Pseudomonas aeruginosa from patients with cystic fibrosis. J Clin Microbiol **42:**1915–1922. http://dx.doi.org/10.1128/JCM.42.5.1915-1922.2004.
16. **O'Toole GA, Kolter R.** 1998. Flagellar and twitching motility are necessary for Pseudomonas aeruginosa biofilm development. Mol Microbiol **30:**295–304. http://dx.doi.org/10.1046/j.1365-2958.1998.01062.x.
17. **Parsek MR, Tolker-Nielsen T.** 2008. Pattern formation in Pseudomonas aeruginosa biofilms. Curr Opin Microbiol **11:**560–566. http://dx.doi.org/10.1016/j.mib.2008.09.015.
18. **Ceri H, Olson ME, Stremick C, Read RR, Morck D, Buret A.** 1999. The Calgary biofilm device: new technology for rapid determination of antibiotic susceptibilities of bacterial biofilms. J Clin Microbiol **37:**1771–1776.
19. **Crusz SA, Popat R, Rybtke MT, Camara M, Givskov M, Tolker-Nielsen T, Diggle SP, Williams P.** 2012. Bursting the bubble on bacterial biofilms: a flow cell methodology. Biofouling **28:**835–842. http://dx.doi.org/10.1080/08927014.2012.716044.
20. **Holloway BW, Morgan AF.** 1986. Genome organization in Pseudomonas. Annu Rev Microbiol **40:**79–105. http://dx.doi.org/10.1146/annurev.mi.40.100186.000455.
21. **Marvig RL, Sommer LM, Molin S, Johansen HK.** 2015. Convergent evolution and adaptation of Pseudomonas aeruginosa within patients with cystic fibrosis. Nat Genet **47:**57–64. http://dx.doi.org/10.1038/ng.3148.
22. **Haagensen J, Klausen M, Ernst R, Miller S, Folkesson A, Tolker-Nielsen T, Molin S.** 2007. Differentiation and distribution of colistin- and sodium dodecyl sulfate-tolerant cells in Pseudomonas aeruginosa biofilms. J Bacteriol **189:**28–37. http://dx.doi.org/10.1128/JB.00720-06.
23. **Clinical and Laboratory Standards Institute.** 2013. Performance standards for antimicrobial susceptibility testing, 23rd informational supplement. CLSI document M100-S23. Clinical and Laboratory Standards Institute, Wayne, PA.
24. **Kuti JL, Dandekar PK, Nightingale CH, Nicolau DP.** 2003. Use of Monte Carlo simulation to design an optimized pharmacodynamic dosing strategy for meropenem. J Clin Pharmacol **43:**1116–1123. http://dx.doi.org/10.1177/0091270003257225.
25. **Grasso S, Meinardi G, de Carneri I, Tamassia V.** 1978. New in vitro model to study the effect of antibiotic concentration and rate of elimination on antibacterial activity. Antimicrob Agents Chemother **13:**570–576. http://dx.doi.org/10.1128/AAC.13.4.570.
26. **Tolker-Nielsen T, Sternberg C.** 2011. Growing and analyzing biofilms in flow chambers. Curr Protoc Microbiol Chapter 1:Unit 1B.2. http://dx.doi.org/10.1002/9780471729259.mc01b02s21.
27. **Heydorn A, Ersbøll BK, Hentzer M, Parsek MR, Givskov M, Molin S.** 2000. Experimental reproducibility in flow chamber biofilms. Microbiology **146:**2409–2415.
28. **Moller S, Sternberg C, Andersen JB, Christensen BB, Ramos JL, Givskov M, Molin S.** 1998. In situ gene expression in mixed-culture biofilms: evidence of metabolic interactions between community members. Appl Environ Microbiol **64:**721–732.
29. **Yang L, Barken KB, Skindersoe ME, Christensen AB, Givskov M, Tolker-Nielsen T.** 2007. Effects of iron on DNA release and biofilm development by Pseudomonas aeruginosa. Microbiology **153:**1318–1328. http://dx.doi.org/10.1099/mic.0.2006/004911-0.
30. **Huang L, Haagensen J, Verotta D, Lizak P, Aweeka F, Yang K.** 2014. Determination of meropenem in bacterial media by LC-MS/MS. J Chromatogr B Analyt Technol Biomed Life Sci **961:**71–76. http://dx.doi.org/10.1016/j.jchromb.2014.05.002.
31. **Lindstrom ML, Bates DM.** 1990. Nonlinear mixed effects models for repeated measures data. Biometrics **46:**673–687. http://dx.doi.org/10.2307/2532087.
32. **Klausen M, Heydorn A, Ragas P, Lambertsen L, Aaes-Jørgensen A, Molin S, Tolker-Nielsen T.** 2003. Biofilm formation by Pseudomonas aeruginosa wild type, flagella and type IV pili mutants. Mol Microbiol **48:**1511–1524. http://dx.doi.org/10.1046/j.1365-2958.2003.03525.x.
33. **Pereira MO, Kuehn K, Wuertz S, Neu T, Melo LF.** 2002. Effect of flow regime on the architecture of a Pseudomonas fluorescens biofilm. Biotechnol Bioeng **78:**164–171. http://dx.doi.org/10.1002/bit.10189.
34. **Shrout JD, Chopp DL, Just CL, Hentzer M, Givskov M, Parsek MR.** 2006. The impact of quorum sensing and swarming motility on Pseudomonas aeruginosa biofilm formation is nutritionally conditional. Mol Microbiol **62:**1264–1277. http://dx.doi.org/10.1111/j.1365-2958.2006.05421.x.
35. **Walters MC, III, Roe F, Bugnicourt A, Franklin MJ, Stewart PS.** 2003. Contributions of antibiotic penetration, oxygen limitation, and low metabolic activity to tolerance of Pseudomonas aeruginosa biofilms to ciprofloxacin and tobramycin. Antimicrob Agents Chemother **47:**317–323. http://dx.doi.org/10.1128/AAC.47.1.317-323.2003.
36. **Blumer JL, Saiman L, Konstan MW, Melnick D.** 2005. The efficacy and safety of meropenem and tobramycin vs ceftazidime and tobramycin in the treatment of acute pulmonary exacerbations in patients with cystic fibrosis. Chest **128:**2336–2346. http://dx.doi.org/10.1378/chest.128.4.2336.
37. **Flume PA, Mogayzel PJ, Jr, Robinson KA, Goss CH, Rosenblatt RL, Kuhn RJ, Marshall BC, Clinical Practice Guidelines for Pulmonary Therapies Committee.** 2009. Cystic fibrosis pulmonary guidelines: treatment of pulmonary exacerbations. Am J Respir Crit Care Med **180:**802–808. http://dx.doi.org/10.1164/rccm.200812-1845PP.
38. **Zobell JT, Young DC, Waters CD, Ampofo K, Cash J, Marshall BC, Olson J, Chatfield BA.** 2011. A survey of the utilization of anti-

pseudomonal beta-lactam therapy in cystic fibrosis patients. Pediatr Pulmonol **46:**987–990. http://dx.doi.org/10.1002/ppul.21467.

39. **Mulcahy LR, Burns JL, Lory S, Lewis K.** 2010. Emergence of Pseudomonas aeruginosa strains producing high levels of persister cells in patients with cystic fibrosis. J Bacteriol **192:**6191–6199. http://dx.doi.org/10.1128/JB.01651-09.
40. **Costerton JW, Lewandowski Z, Caldwell DE, Korber DR, Lappin-Scott HM.** 1995. Microbial biofilms. Annu Rev Microbiol **49:**711–745. http://dx.doi.org/10.1146/annurev.mi.49.100195.003431.
41. **Bagge N, Schuster M, Hentzer M, Ciofu O, Givskov M, Greenberg EP, Hoiby N.** 2004. Pseudomonas aeruginosa biofilms exposed to imipenem exhibit changes in global gene expression and beta-lactamase and alginate production. Antimicrob Agents Chemother **48:**1175–1187. http://dx.doi.org/10.1128/AAC.48.4.1175-1187.2004.
42. **Bjarnsholt T, Jensen PO, Burmolle M, Hentzer M, Haagensen JA, Hougen HP, Calum H, Madsen KG, Moser C, Molin S, Hoiby N, Givskov M.** 2005. Pseudomonas aeruginosa tolerance to tobramycin, hydrogen peroxide and polymorphonuclear leukocytes is quorum-sensing dependent. Microbiology **151:**373–383. http://dx.doi.org/10.1099/mic.0.27463-0.
43. **Pamp SJ, Gjermansen M, Johansen HK, Tolker-Nielsen T.** 2008. Tolerance to the antimicrobial peptide colistin in Pseudomonas aeruginosa biofilms is linked to metabolically active cells, and depends on the pmr and mexAB-oprM genes. Mol Microbiol **68:**223–240. http://dx.doi.org/10.1111/j.1365-2958.2008.06152.x.
44. **Bagge N, Hentzer M, Andersen JB, Ciofu O, Givskov M, Hoiby N.** 2004. Dynamics and spatial distribution of beta-lactamase expression in Pseudomonas aeruginosa biofilms. Antimicrob Agents Chemother **48:**1168–1174. http://dx.doi.org/10.1128/AAC.48.4.1168-1174.2004.
45. **Islam S, Oh H, Jalal S, Karpati F, Ciofu O, Hoiby N, Wretlind B.** 2009. Chromosomal mechanisms of aminoglycoside resistance in Pseudomonas aeruginosa isolates from cystic fibrosis patients. Clin Microbiol Infect **15:**60–66. http://dx.doi.org/10.1111/j.1469-0691.2008.02097.x.
46. **Jalal S, Ciofu O, Hoiby N, Gotoh N, Wretlind B.** 2000. Molecular mechanisms of fluoroquinolone resistance in Pseudomonas aeruginosa isolates from cystic fibrosis patients. Antimicrob Agents Chemother **44:**710–712. http://dx.doi.org/10.1128/AAC.44.3.710-712.2000.
47. **Poole K.** 2007. Efflux pumps as antimicrobial resistance mechanisms. Ann Med **39:**162–176. http://dx.doi.org/10.1080/07853890701195262.
48. **MacGowan A, Bowker K.** 2002. Developments in PK/PD: optimising efficacy and prevention of resistance. A critical review of PK/PD in in vitro models. Int J Antimicrob Agents **19:**291–298. http://dx.doi.org/10.1016/S0924-8579(02)00027-4.
49. **White RL.** 2001. What in vitro models of infection can and cannot do. Pharmacotherapy **21:**292S–301S. http://dx.doi.org/10.1592/phco.21.18.292S.33906.